Supplementary Information (SI) for Inorganic Chemistry Frontiers.
This journal is © the Partner Organisations 2026

Supplementary Information

An Ir(III)-based Type I Photosensitizer Triggers Immunogenic Pyroptosis in Prostate Cancer

Tianyi Kang, ‡ Fangfang Wei, ‡ Yuxin Shi, ‡ Jiayuan Xu, Jiqiang Liu, Boyan Huang, Mingcheng Liu, Jin-Tang Dong, Li Zhou, Keith Man-Chung Wong, Kai Li**

Experimental Section

Materials and Reagents: All solvents utilized in synthesis were of analytical grade. Commercial chemicals were used as received: Iridium(III) chloride hydrate and 4,4'-dimethyl-2,2'-bipyridine were procured from Aldrich Chemical Company; 2,3-diphenylpyrazine and dibenzo[f,h]quinoxaline were acquired from Meyer Chemical Company; 1,2-di(thiophen-2-yl)ethane-1,2-dione was a product of Sigma-Aldrich Chemical Company. The dinuclear precursors $[Ir(C^N)_2Cl]_2$ [54-56] and the **Fluo-bpy** ligand [46] were prepared following previously described methodologies. Cell culture media and supplements—Roswell Park Memorial Institute 1640 (RPMI 1640), fetal bovine serum (FBS), penicillin-streptomycin solution, and phosphate-buffered saline (PBS, 1×)—were supplied by Viva Cell and Biosharp, respectively. DCFH-DA was bought from Aladdin Reagent Co., Ltd. HPF and DHE were products from McLyn Biochemical Technology Co., Ltd. ABDA was purchased from MaoKang Biotechnology Co., Ltd. SOSG was purchased from MeilunBio Co., Ltd. $CoCl_2$ was purchased from HARVEYBIO. ELISA kits of IL-6, TNF-α, IL-18, IL-1β, IL-10 and IFN-γ were bought from Beijing 4A Biotech Co., Ltd and Multi Sciences separately. GSDMD and Caspase-1 antibodies for WB are commercial products from Cell Signaling Technology, Inc. β-actin antibody for WB, HMGB1 and Calreticulin antibody for immunostaining were obtained from Abcam. All antibodies for flowcytometry analysis (anti-CD86-FITC, anti-CD11c-PE, anti-CD80-APC, anti-CD45-blue, anti-CD8-PE, anti-CD3-FITC and anti-CD4-APC) were purchased from Biolegend. PI/Annexin V assay kit, Cell Counting Kit-8 (CCK-8), LDH cytotoxicity

detection kit, ATP assay kit, BCA assay kit, VX-765 and Z-VAD-FMK were purchased from Beyotime Biotechnology. TMRE was bought from MedChemExpress.

Physical Measurements and Instrumentations: The room-temperature electronic absorption and emission measurements are carried out on Agilent Cary 60 UV–vis spectrophotometer and Edinburgh instruments FLS980 and FS5 fluorescence spectrometers. The time-resolved transient absorption spectra are recorded on Edinburgh laser flash photolysis instrument LP920. Quartz cuvettes with 1 cm path length are utilized in all photophysical measurements. All solutions for time-resolved transient absorption measurements are strictly de-aerated for four cycles *via* successive freeze–pump–thaw process. The absolute photoluminescence quantum yields are measured on Hamamatsu instrument C11347. Nuclear magnetic resonance (NMR) measurements are conducted on Bruker AVANCE 400 (^{1}H NMR for 400 MHz and ^{13}C{^{1}H} NMR for 100 MHz) or Bruker AVANCE 500 (^{1}H NMR for 500 MHz and ^{13}C{^{1}H} NMR for 126 MHz) Fourier transform NMR spectrometers, and the internal standard is TMS [$(CH_3)_4Si$] for chemical shifts in NMR spectra. Orbitrap Fusion Tribrid mass spectrometer is employed to collect high-resolution mass spectra.

Synthesis:

Ir1: **[Ir(dpp)$_2$Cl]$_2$** was combined with two equivalents of **Fluo-bpy** in a mixed solvent of dichloromethane and methanol (1:1, v/v). The reaction vessel was protected from light and maintained under a nitrogen atmosphere while being refluxed for 12 hours. After cooling to room temperature, the solution was concentrated under reduced pressure. Purification was carried out by column chromatography on silica gel, eluting with a gradient of DCM and methanol (20:1, v/v), affording the desired complex as a dark purple powder. **Yield**: 77 mg (53%).

^{1}H NMR (500 MHz, DMSO) δ 9.04 (d, *J* = 12.9 Hz, 2H), 8.46 – 8.38 (m, 2H), 8.13 (d, *J* = 3.3 Hz, 1H), 7.91 (dd, *J* = 9.7, 4.4 Hz, 2H), 7.84 (d, *J* = 5.6 Hz, 1H), 7.69 (d, *J* = 5.7 Hz, 1H), 7.64 – 7.60 (m, 10H), 7.02 (d, *J* = 9.4 Hz, 1H), 6.98 – 6.95 (m, 2H), 6.86 – 6.81 (m, 2H), 6.73 – 6.69 (m, 2H), 6.53 – 6.50 (m, 2H), 6.37 (d, *J* = 7.3 Hz, 1H), 6.19 (dd, *J* = 9.4, 2.1 Hz, 1H), 6.05 – 6.01 (m, 4H), 1.77 (s, 3H). ^{13}C NMR (151 MHz,

DMSO) δ 160.02, 159.77, 157.25, 156.50, 155.36, 153.91, 153.73, 152.77, 152.61, 152.54, 151.03, 150.90, 149.81, 146.20, 145.17, 143.94, 143.87, 143.79, 143.63, 142.73, 142.54, 142.41, 142.35, 142.22, 142.14, 138.98, 131.50, 131.30, 131.20, 130.78, 130.33, 130.14, 129.64, 129.27, 129.22, 127.17, 126.49, 126.30, 124.64, 123.84, 122.36, 122.17, 118.56, 104.13, 21.30. HRMS (ESI): theoretical calc. for $C_{56}H_{37}IrN_6O_3$ $[M+H]^+$ m/z = 1035.2629, found $[M+H]^+$ m/z = 1035.2665.

Ir2: This complex was obtained by adopting an analogous synthetic route to **Ir1**, wherein **$[Ir(dpz)_2Cl]_2$** was used as the metal precursor instead of **$[Ir(dpp)_2Cl]_2$**. Purification of the crude material by column chromatography over silica gel, eluted with DCM/methanol (20:1, v/v), yielded the pure product as a dark purple powder. **Yield**: 78 mg (54%).

^{1}H NMR (500 MHz, CD_3CN) δ 9.27 (d, *J* = 8.1 Hz, 2H), 8.84 (d, *J* = 3.0 Hz, 1H), 8.80 (d, *J* = 3.1 Hz, 1H), 8.75 (dd, *J* = 8.2, 2.9 Hz, 2H), 8.61 (s, 1H), 8.48 (s, 1H), 8.30 (d, *J* = 3.0 Hz, 1H), 8.27 (d, *J* = 8.2 Hz, 2H), 8.16 (d, *J* = 5.5 Hz, 1H), 8.07 (d, *J* = 3.0 Hz, 1H), 7.96 – 7.93 (m, 2H), 7.89 – 7.86 (m, 3H), 7.45 (d, *J* = 5.6 Hz, 1H), 7.35 – 7.31 (m, 3H), 7.08 (d, *J* = 9.3 Hz, 1H), 6.61 (dd, *J* = 8.3, 3.1 Hz, 2H), 6.56 (d, *J* = 7.3 Hz, 1H), 6.34 (dd, *J* = 9.3, 2.1 Hz, 1H), 6.16 (d, *J* = 2.1 Hz, 1H), 6.11 (d, *J* = 2.1 Hz, 1H), 6.07 (dd, *J* = 9.3, 2.1 Hz, 1H), 2.51 (s, 3H). ^{13}C NMR (151 MHz, DMSO) δ 156.32, 155.71, 155.14, 154.69, 151.61, 151.43, 150.75, 150.49, 149.55, 148.43, 148.03, 147.93, 145.33, 145.21, 143.89, 143.12, 142.74, 142.24, 141.81, 141.63, 137.12, 136.91, 131.78, 131.39, 130.80, 130.30, 129.53, 129.05, 128.96, 128.89, 128.78, 128.69, 128.60, 128.43, 128.00, 127.93, 127.72, 127.22, 126.39, 125.77, 125.20, 124.90, 124.22, 123.42, 123.03, 115.96, 115.79, 103.02, 20.15. HRMS (ESI): m/z theoretical calc. for $C_{56}H_{33}IrN_6O_3$ $[M+H]^+$ m/z = 1031.2316, found $[M+H]^+$ m/z = 1031.2343.

Ir3: This compound was prepared according to the procedure for **Ir1**. The only modification was the use of **$[Ir(dtqx)_2Cl]_2$** in place of **$[Ir(dpp)_2Cl]_2$**. The crude product was purified via column chromatography on silica gel eluting with DCM/methanol (20:1, v/v), yielding the product as a dark purple powder. **Yield**: 76 mg (62%).

^{1}H NMR (600 MHz, DMSO) δ 8.63 (d, *J* = 29.5 Hz, 2H), 8.40 (d, *J* = 5.6 Hz, 1H), 8.18 (d, *J* = 5.8 Hz, 1H), 8.04 – 7.98 (m, 5H), 7.94 (d, *J* = 3.3 Hz, 1H), 7.90 (d, *J* = 3.5 Hz, 1H), 7.82 (d, *J* = 5.9 Hz, 1H), 7.70 (t, *J* = 7.6 Hz, 1H), 7.63 (t, *J* = 7.6 Hz, 1H), 7.59 (d, *J* = 4.9 Hz, 2H), 7.43 – 7.37 (m, 2H), 7.35 – 7.33 (m, 1H), 7.29 – 7.22 (m, 2H), 7.03 (d, *J* = 8.9 Hz, 1H), 6.68 (d, *J* = 9.4 Hz, 1H), 6.33 (dd, *J* = 11.9, 4.9 Hz, 2H), 6.22 (d, *J*

= 9.4 Hz, 1H), 6.04 (s, 1H), 6.00 (s, 1H), 5.95 (d, *J* = 10.4 Hz, 1H), 5.87 (d, *J* = 9.3 Hz, 1H), 2.45 (s, 3H). ^{13}C NMR (126 MHz, DMSO) δ 181.22, 161.86, 160.37, 157.54, 156.41, 155.06, 153.37, 149.03, 148.08, 147.35, 147.10, 147.02, 144.15, 141.24, 141.17, 139.56, 139.50, 138.37, 138.08, 137.71, 136.32, 136.23, 133.35, 132.32, 132.05, 131.98, 130.91, 130.84, 130.48, 130.34, 130.19, 130.11, 129.77, 129.68, 129.54, 129.30, 128.75, 127.98, 126.44, 125.27, 124.64, 124.44, 122.87, 122.73, 107.19, 107.12, 104.14, 104.09, 21.22. HRMS (ESI): m/z theoretical calc. for $C_{56}H_{33}IrN_6O_3S_4$ $[M+H]^+$ m/z = 1159.1199, found $[M+H]^+$ m/z = 1159.1228.

Computational Studies: We performed all density functional theory (DFT) calculations with the Gaussian 16 program. [57] We optimized all geometries in the gas phase using the hybrid generalized gradient approximation functional B3LYP [58-61] and the double-ζ valence def2-SVP basis set [62] for all elements. To incorporate aqueous solvation effects on the computed Gibbs energy profile, we conducted single-point calculations employing the triple-ζ valence basis set def2-TZVP [63] combined with the SMD continuum solvation model [64] with intrinsic atomic Coulomb radii for water (ε = 78.3553). We applied Grimme's dispersion correction D3 method to both optimization and single-point calculations. [65] We confirmed all local minimum structures through vibrational frequency analysis, verifying the absence of imaginary frequencies. We prepared all molecular images using VMD [66] and Multiwfn [67] software. The spin orbit coupling (SOC) values were calculated using TDDFT method at the level of B3LYP/DKH-def2-TZVP, with level of SARC-DKH-TZVP for Ir, performed by ORCA 5.0. [68]

Cell Viability: For the dark toxicity assay of different photosensitizers, RM-1 cells were seeded in a 96-well plate at a density of 7×10^3 cells per well and allowed to adhere for 24 hours. Subsequently, the cells were treated with different concentrations (0.3125–10 μM) of Ir1-Ir3 molecules. Following a 24-hour incubation, cell viability was assessed using the Cell Counting Kit-8 (CCK-8) assay.

In parallel, the photo-dark toxicity of the compounds was evaluated on RM-1 cells that pre-seeded in 96-well plates. After 24 h, they were incubated with Ir1-Ir3

molecules at the same gradient concentrations in the dark toxicity assay. Upon 6 h incubation, RM-1 cells were immediately irradiated under white light (10 mW cm^{-2}) for 5 min. The culture medium was retained for a further 24 h incubation in a lightproof environment at 37°C until the CCK-8 test was conducted.

ROS Measurements of Ir1-Ir3 Molecules:

(1) Hydroxyl Radicals: Hydroxyl radicals were detected by the specific •OH indicator hydroxyphenyl fluorescein (HPF). [69] HPF can be oxidized by •OH to form fluorescein and emits intense fluorescence at 515 nm. The emission spectra were recorded at an excitation of 488 nm and the relative emission intensity (I/I_0) at 515 nm versus irradiation time was then plotted.

(2) Superoxide Anion: Superoxide anion radicals were detected by the specific $O_2^{\bullet-}$ indicator dihydrorhodamine 123 (DHR 123). [70] DHR 123 can be oxidized by $O_2^{\bullet-}$ to form DHR and emits intense fluorescence at 527 nm. The emission spectra were recorded at an excitation of 488 nm and the relative emission intensity (I/I_0) at 527 nm versus irradiation time was then plotted.

(3) Singlet Oxygen: The $^1O_2$ generation of complexes has been measured according to the reported protocols using 9,10-anthracenediyl-bis(methylene)dimalonic acid (ABDA, Sigma-Aldrich) as a $^1O_2$ indicator. [71, 72] ABDA and the complex were prepared in air-saturated water with their absorbances adjusted to 0.4 at 378 nm and 0.1 at 400 nm, respectively. The photo-oxidation of ABDA was then monitored at specified intervals under irradiation at 500 nm using a Xenon lamp equipped with an external air-cooling system. The irradiance of the light source was standardized to 2 mW cm^{-2} by adjusting the source-to-sample distance, as quantified by an optical power meter (PM100D, Thorlabs) employing the standard 5-point method.

(4) Total ROS: Prior to the assay, DCFH-DA (0.5 mL, 1 mM in ethanol) was hydrolyzed in NaOH (2 mL, 0.01 M) for 30 min at room temperature. The mixture was subsequently neutralized with sodium phosphate buffer (10 mL, 25 mM, pH 7.4) and stored in the dark at 4°C to obtain the active DCFH solution (40 μM). For the detection, an aliquot of this solution (2 mL) was mixed with the Ir(III) complexes (10 μL, 100 μM in DMSO). The formation of fluorescent DCF upon white light irradiation (2 mW cm^{-2})

was monitored by recording emission spectra (480 nm), and the relative intensity at 525 nm (I/I_0) was plotted against irradiation time. [73]

ROS Detection at the Cellular Level in Normoxia and Hypoxia: Different from the normoxia group, cells in the hypoxia group were pre-treated with $CoCl_2$ (250 nM) for 12 h. Then the following process was the same. RM-1 cells (3×10^3 cells/well) were pre-dispersed on confocal dishes, then divided into 3 groups: PBS, Ir3 and Ir3+Light. As for the Ir3 and Ir3+Light groups, cells experienced 6 h-incubation with Ir3 molecules at the concentration of 5 μM. DCFH-DA, HPF, DHE and SOSG probes were diluted at a 1:1000 dilution ratio using serum-free 1640 medium and incubated with cells at 37℃ for 30 min. As for Ir3+Light group, cells were irradiated with white light (10 mW cm^{-2}, 5 min) upon 30 min incubation with DCFH-DA. Finally, all the groups were imaged with CLSM after three times washes with 1×PBS.

Western Blotting Assay: RM-1 cells were pre-seeded in 6-well plates at a density of 2×10^6 cells/well and divided into four groups: PBS, PBS+Light, Ir3 and Ir3+Light. After 24 h, the cell culture medium of Ir3 and Ir3+Light groups was replaced with medium containing 5 μM concentration of Ir3 molecules and incubated for another 6 h. Subsequently, cells in PBS+Light and Ir3+Light groups were irradiated with white light (10 mW cm^{-2}, 5 min), followed by continued incubation for 12 h. Then, cells in all groups were individually collected for the detection of total protein by BCA assay. After electrophoresis, transmembrane and blocking processes, the PVDF membrane which was transferred with protein samples, was subsequently incubated with the primary antibodies (including GSDMD, Caspase-1, and β-actin) and the HRP-conjugated secondary antibody one after the other. The images of target proteins were captured using a Bio-Rad ChemiDoc XRS Chemiluminescence Imaging System. The data were analyzed using Image J software.

Caspase-1 and Caspase-3 Pathway Study: RM-1 cells (7×10^3 cells/well) were pre-inoculated in 96-well plates for 24 h, then they were divided into two groups and both were co-incubated with gradient concentrations of Ir3 molecules (0.3125, 0.625, 1.25, 2.5, 5, and 10 μM). In one of the groups, VX-765 (10 μM) or Z-VAD-FMK (10 μM) was added into the culture medium to block the protein activity of Caspase-1 or

Caspase-3. 6 h later, RM-1 cells were irradiated under white light conditions (10 mW cm^{-2}, 5 min). after a further 24 h of incubation, a CCK-8 assay was performed.

Lactate Dehydrogenase (LDH) and Cytokines Release Assays: For LDH and IL-18/IL-1β cytokine release assays, RM-1 cells were pre-seeded into 24-well plates (3×10^4 cells/well) for 24 h and divided into four groups: PBS, PBS+Light, Ir3 and Ir3+Light. Cells in Ir3 and Ir3+Light groups were pre-treated with Ir3 solution (5 μM) for 6 h. Then, the cells in PBS+Light and Ir3+Light groups were exposed to white light (10 mW cm^{-2}, 5 min), followed by 24 h incubation. We employed a commercially available LDH cytotoxicity detection kit to quantify the LDH activity in the cell culture supernatant. Meanwhile, the IL-18 and IL-1β release were measured using their corresponding ELISA kits.

ATP Release Assay: As for the ATP release assay, the cell treatment step is the same as the LDH release assay except that the incubation time after irradiation was reduced from 24 h to 12 h. The adherent cells and cellular supernatants were collected separately to detect ATP content using an ATP assay kit.

Cellular Apoptosis by Flow Cytometry: We conducted flow cytometry analysis on pretreated RM-1 cells. Briefly, cells were plated in 12-well plates at 1×10^6 cells/well and received the indicated treatments (PBS, PBS+Light, Ir3, Ir3+Light). At 2 h after light irradiation (10 mW cm^{-2}, 5 min), we harvested the cells. Prior to analysis, cells underwent twice washes with 1×PBS and were stained following the Annexin V-FITC Apoptosis Detection Kit manufacturer's instructions.

Immunofluorescence Staining for ICD Determination: Prior to treatment, RM-1 cells were planted in confocal dishes (3×10^3 cells/well) for 24 h and assigned to four groups (PBS, PBS+Light, Ir3, Ir3+Light). The Ir3 and Ir3+Light groups were treated with 2.5 μM Ir3 for 6 h. Following this, the PBS+Light and Ir3+Light groups were irradiated with white light (10 mW cm^{-2}, 5 min) and then incubated for an additional 4 h. Cells prepared for immunofluorescence were fixed in 4% paraformaldehyde and subsequently permeabilized with 0.3% Triton X-100. Following this, non-specific binding sites were blocked by incubation with 5% BSA. Overnight incubation at 4 °C with primary antibodies (HMGB1 and Calreticulin, 1:1000 dilution in 3% BSA) was

performed, followed by a 1-hour incubation at room temperature with appropriate secondary antibodies (anti-rabbit and anti-mouse, respectively). After nuclear staining with DAPI, images were acquired using a confocal laser scanning microscope.

Detection of the Mitochondrial Membrane Potential: To explore the variation in mitochondrial membrane potential, RM-1 cells were pre-seeded in 12-well plates (1×10^6 cells/well) and divided into four groups: PBS, PBS+Light, Ir3 and Ir3+Light. Then the medium of Ir3 and Ir3+Light groups was replaced with Ir3 solution (5 μM) for 6 h-incubation. Subsequently, the cells in PBS+Light and Ir3+Light groups were irradiated with white light (10 mW cm^{-2}, 5 min). Then, PBS dilution containing TMRE (5 μM) was added to the plate, which was kept at 37°C away from light. After 2 hours, each group of cells in the plate was collected and prepared into a single-cell suspension. Finally, the TMRE fluorescence expression was detected by flow cytometry to assess potential changes in the mitochondrial membrane.

ICP-MS Assay: The subcellular distribution of Ir3 was studied mainly according to reported procedures. Briefly, RM-1 cells were treated with Ir3 (5 μM) for 12 h. After incubation, the cells were washed and collected in PBS. Mitochondrial, nuclear, and cytoplasmic fractions were isolated from Ir3-treated cells using a commercial cell fractionation kit (Abcam, ab109719) according to the manufacturer's instructions. The concentrations of iridium in these fractions were determined by ICP-MS. Cells cultured in the absence of Ir3 were used as the control.

In Vitro BMDCs Maturation Study: Bone marrow cells were isolated from 6-week-old male C57BL/6 mice on day 0 using a standard protocol. To promote differentiation into bone marrow-derived dendritic cells (BMDCs), the cells were maintained in culture medium supplemented with GM-CSF (10 ng/mL) and IL-4 (5 ng/mL). To assess the immunogenic cell death (ICD) effect induced by PDT, the immature BMDCs were co-cultured with PDT-treated tumor cells starting on day 3 of the induction process.

On the other hand, RM-1 tumor cells (8×10^3 cells/well) were pre-planted onto the @Transwell chambers (5 μm pore-size) for 24 h. Then, RM-1 tumor cells were divided into 4 groups: PBS, PBS+Light, Ir3 and Ir3+Light. The medium of Ir3 and Ir3+Light

groups was added with Ir3 solution (5 μM) for 6 h-incubation, followed by light irradiation (10 mW cm^{-2}, 5 min) on PBS+Light and Ir3+Light groups. Then, the @Transwell chambers loaded with RM-1 tumor cells were immediately translocated onto the 24-well plates which were planted with BMDCs. After 24 h of coincubation, the BMDCs in the lower chamber were collected by centrifugation. Then the single-cell suspension was prepared after staining with the configured CD11c, MHCII and CD86 antibody solutions on ice for 10 min under dark light and washing with PBS once.

The supernatants were collected for the detection of TNF-α, IL-6 and IL-10 levels, following the corresponding ELISA kits. The resulting cell supernatant was centrifuged (4 ℃, 1200 rpm, 3 min) to ensure that it was free of cellular debris. 100 μL of cell supernatant was added to the wells together with the prepared biotinylated antibody working solution and reacted for 90 min at room temperature to ensure adequate reaction with the antibody coated on the wells. Subsequently, each well was washed four times with 300 μL of washing solution, and the last time was patted dry on a thick absorbent paper. The plates were then washed again 4 times after adding the enzyme-conjugated working solution for 30 min at room temperature. 100 μL of the colour developer was added to all wells, and the reaction was carried out for 10 min at room temperature and protected from light before adding the termination solution. After mixing, OD450 was measured immediately.

In Vivo Antitumor Study: A prostate cancer subcutaneous model was established in C57BL/6 mice via injection of RM-1 cells (1×10^5 cells in 100 μL) into the right flank. Upon reaching a tumor volume of approximately 30 mm^3, the mice were randomly assigned to four groups (n=4 per group): (i) PBS, (ii) PBS + Light (150 mW cm^{-2}, 10 min), (iii) Ir3 (1 mg/mL, 50 μL, 2 mg/kg), and (iv) Ir3 + Light (150 mW cm^{-2}, 10 min). The mice received intratumoral injections of PBS or the **Ir3** solution on day 0. Subsequently, groups (ii) and (iv) were subjected to white light irradiation on day 0 and day 4 post-injection. Tumor volumes and body weights were recorded every other day for a duration of 10 days, with digital photographs of the tumors also taken. The

experiment was terminated when the tumor volume reached a humane endpoint of 2000 mm^3.

Immunological Analysis: At the end of *in vivo* treatment, the mice's lymph nodes, spleen and blood were obtained from each group for immunological analysis. To detect immune cells in lymph nodes and spleens, single cell suspension of organs needs to be obtained. Specifically, lymph nodes and spleens were first ground with the aid of a copper mesh, then homogenized using a filter of 70 μm pore size. After obtaining the single cell suspension of spleen, RBC lysis buffer was further applied to remove erythrocytes in cell suspension. Subsequently, the obtained single cells were stained with different biomarkers for the flow cytometry analysis. The maturation degree of DCs in lymph nodes was detected using anti-CD11c-PE, anti-CD86-FITC and anti-CD80-APC according to standard protocols. Anti-CD45-blue, anti-CD3-FITC, anti-CD8-PE, and anti-CD4-APC antibodies were used to detect T-lymphocyte subsets in the spleen.

To detect the levels of inflammation-related cytokines in blood, serum was first isolated following the standard process from the whole blood. Then, the levels of TNF-α, IL-6, and IFN-γ were determined using the corresponding ELISA kits, respectively.

Rechallenge Study: A primary subcutaneous tumor was induced in the right flank of C57BL/6 mice via injection of 5×10^4 RM-1 cells in 100 μL; this cell density was ethically mandated to prevent excessive tumor burden in control cohorts. Upon reaching a volume of 20 mm^3, the primary tumors were subjected to intratumoral administration of Ir3 coupled with light irradiation on days 0 and 2. A secondary tumor challenge on the contralateral flank, using 1×10^5 RM-1 cells in 100 μL, was initiated on day 4. Continuous monitoring of the secondary tumor growth was performed at 48-hour intervals.

Statistics: GraphPad Prism software was employed for statistical analysis. Group differences were analyzed using the Student's t-test. A *P*-value of less than 0.05 was considered statistically significant, with $P < 0.01$ and $P < 0.001$ representing higher levels of significance.

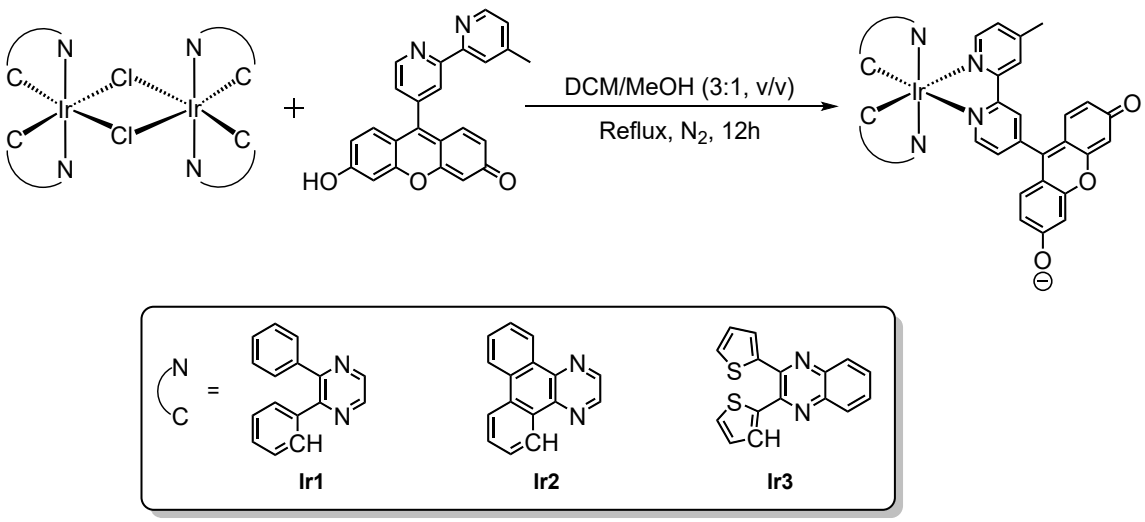

Scheme 1. The synthetic route of target **Ir1**–**Ir3**.

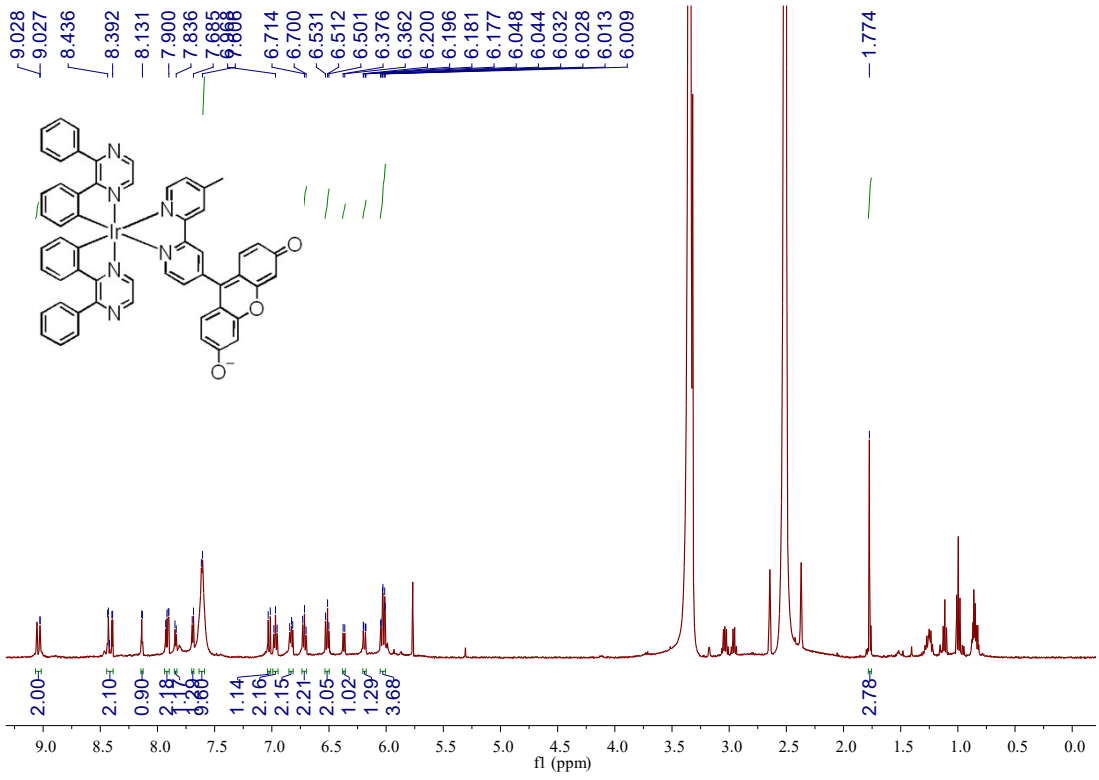

Figure S1. ^{1}H NMR spectrum of **Ir1**.

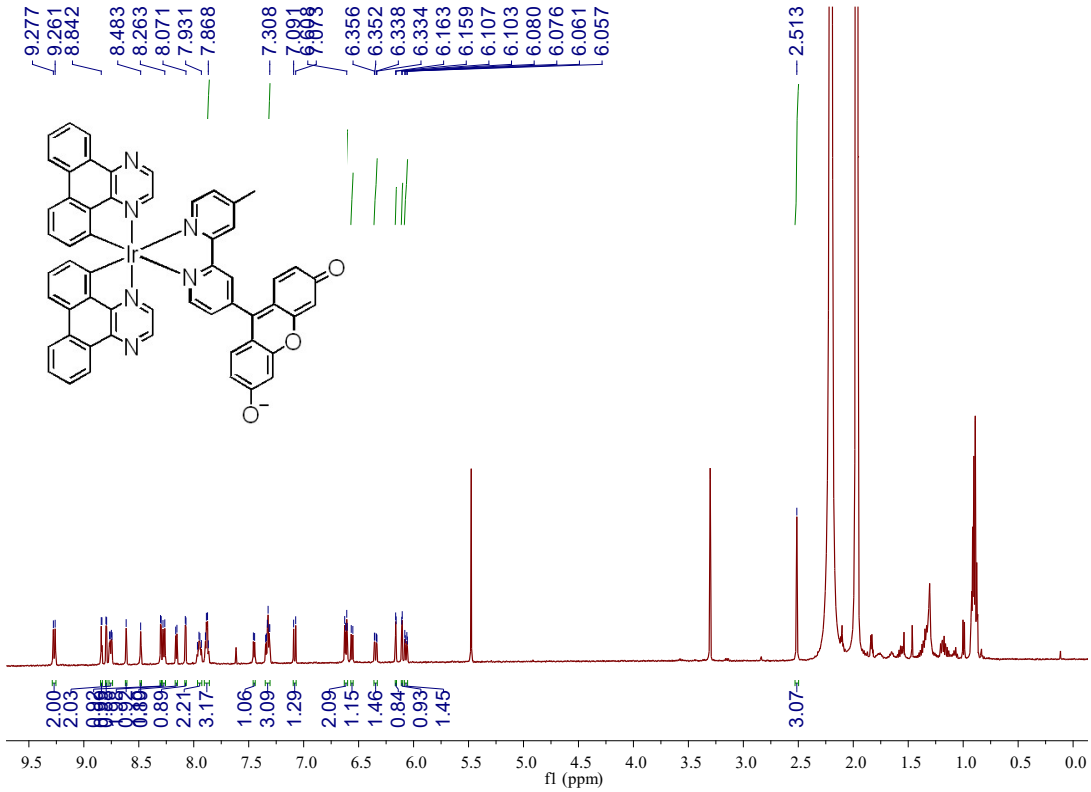

Figure S2. [1]H NMR spectrum of **Ir2**.

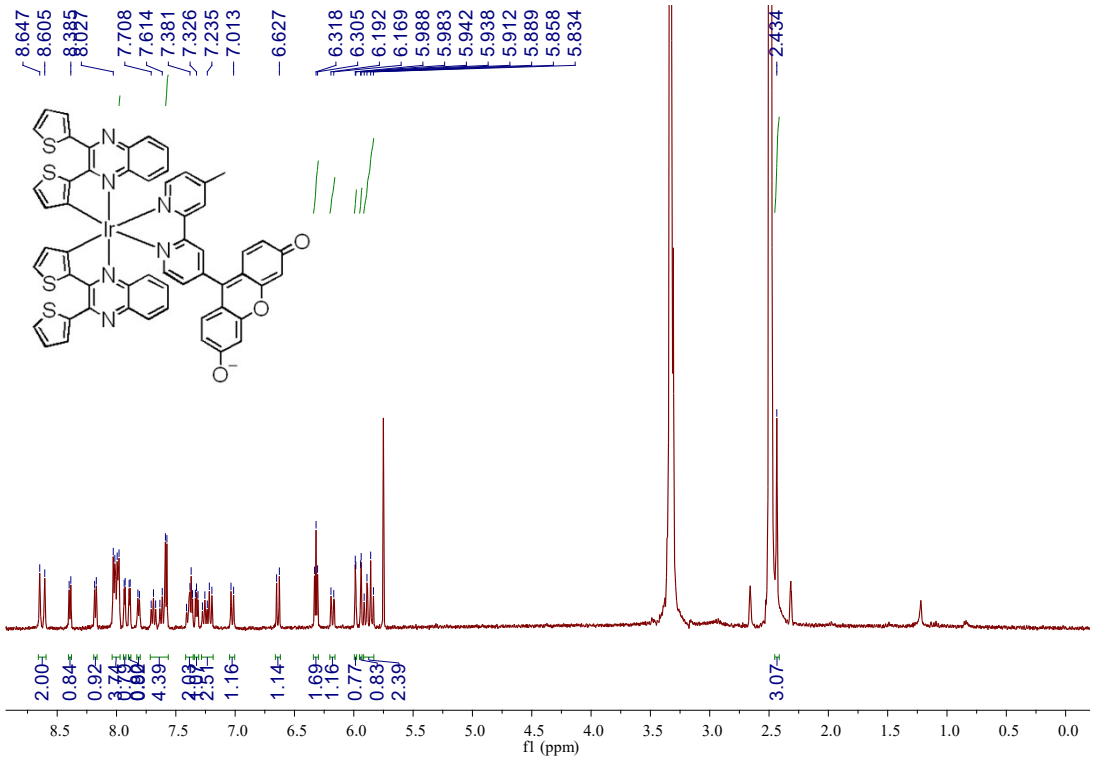

Figure S3. [1]H NMR spectrum of **Ir3**.

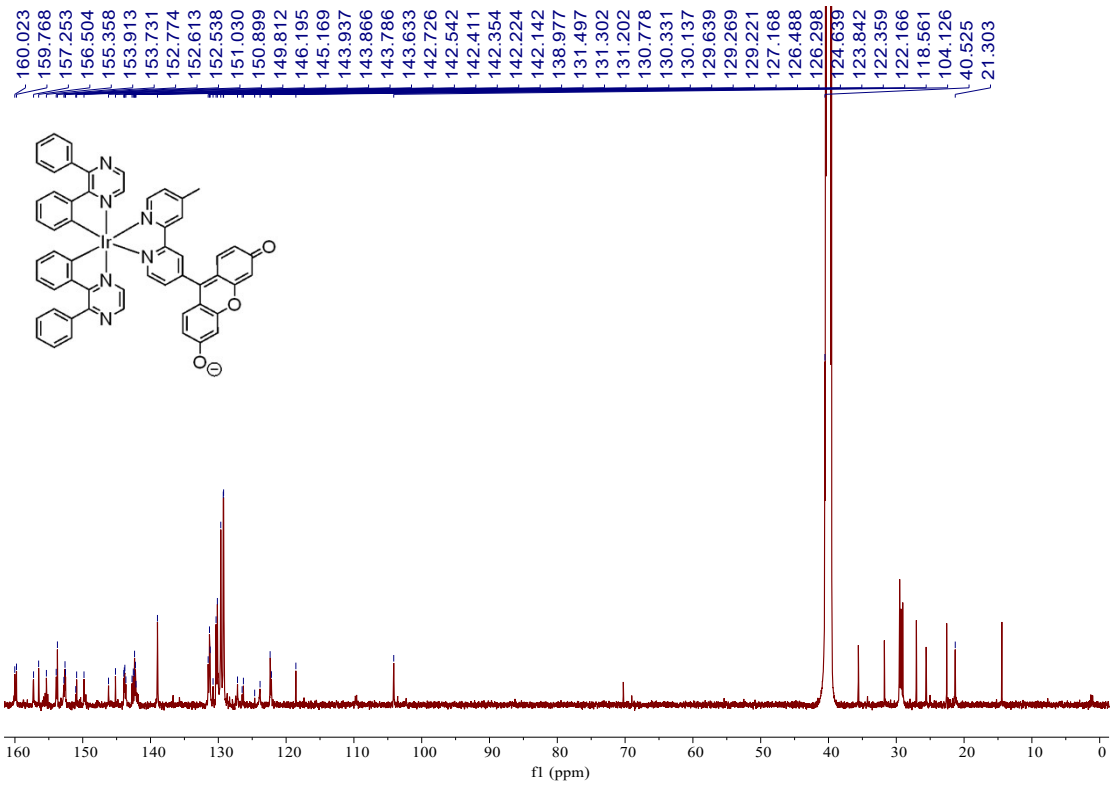

Figure S4. ^{13}C NMR spectrum of **Ir1**.

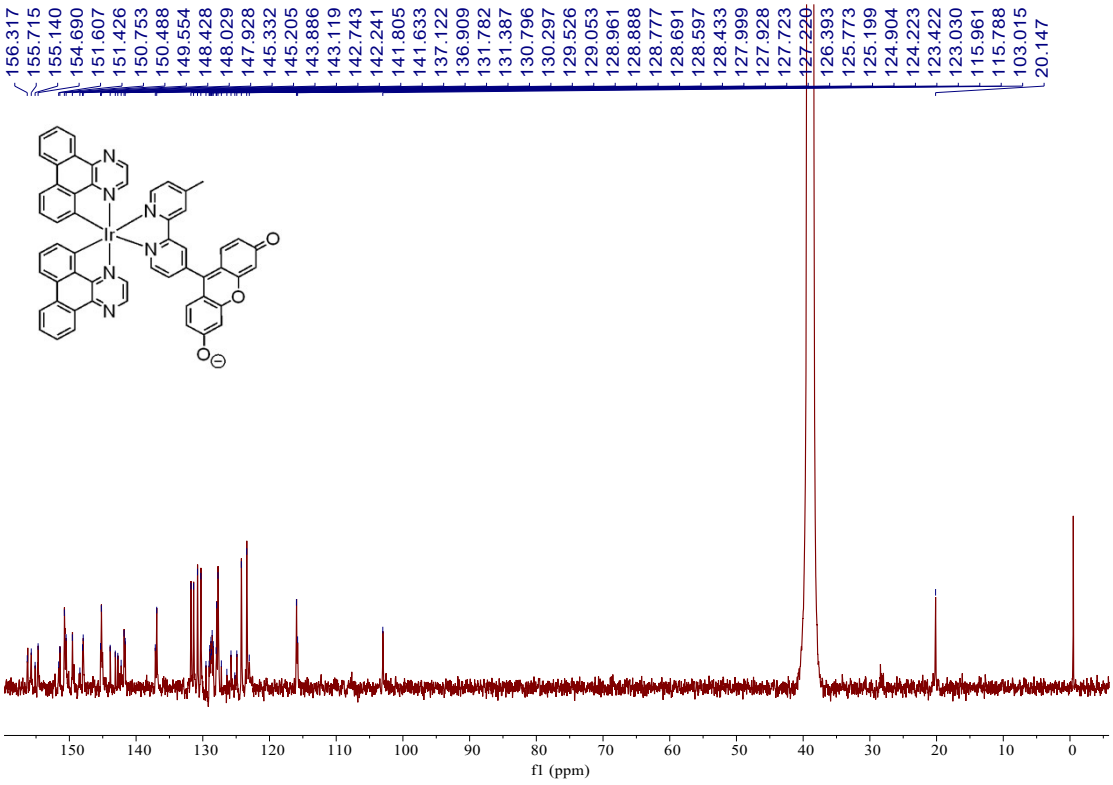

Figure S5. ^{13}C NMR spectrum of **Ir2**.

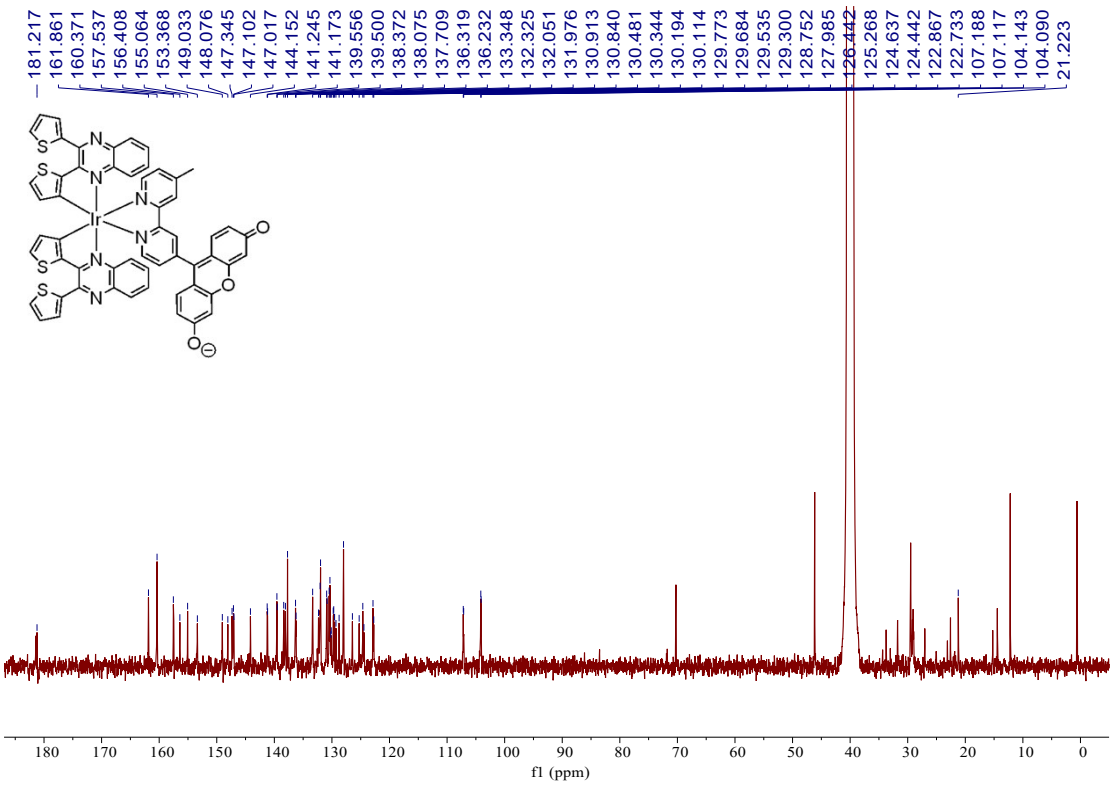

Figure S6. ^{13}C NMR spectrum of **Ir3**.

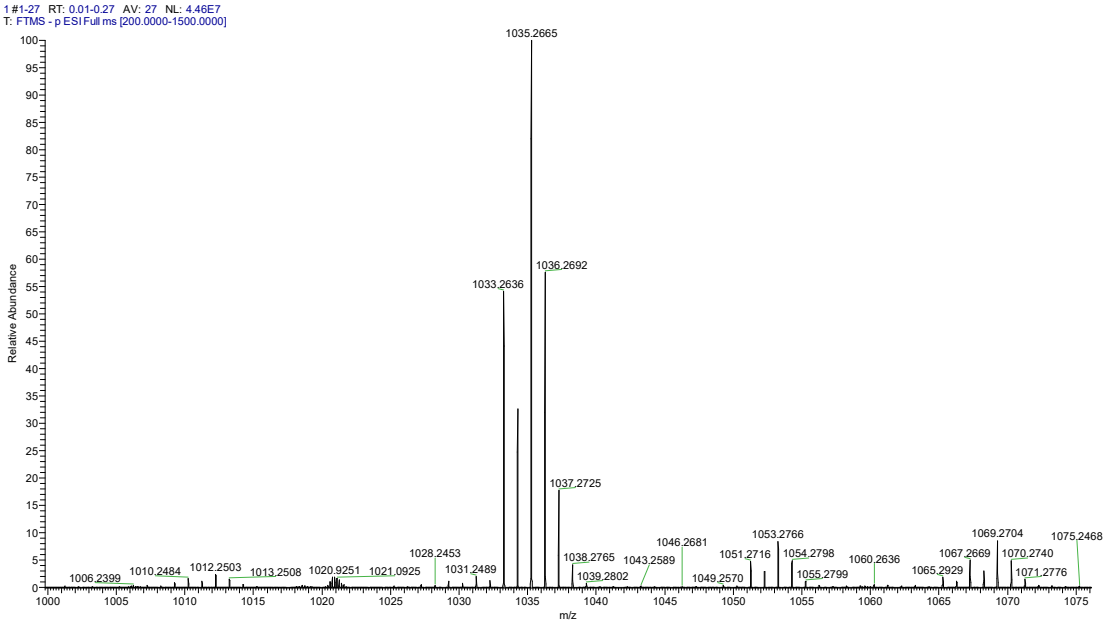

Figure S7. HRMS spectrum of **Ir1**.

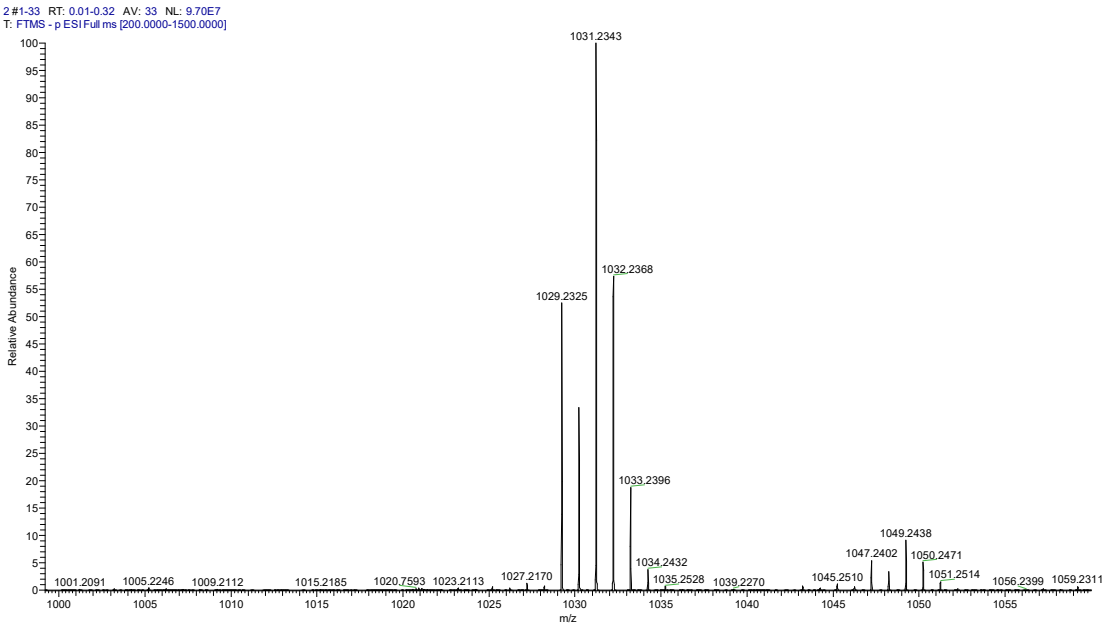

Figure S8. HRMS spectrum of **Ir2**.

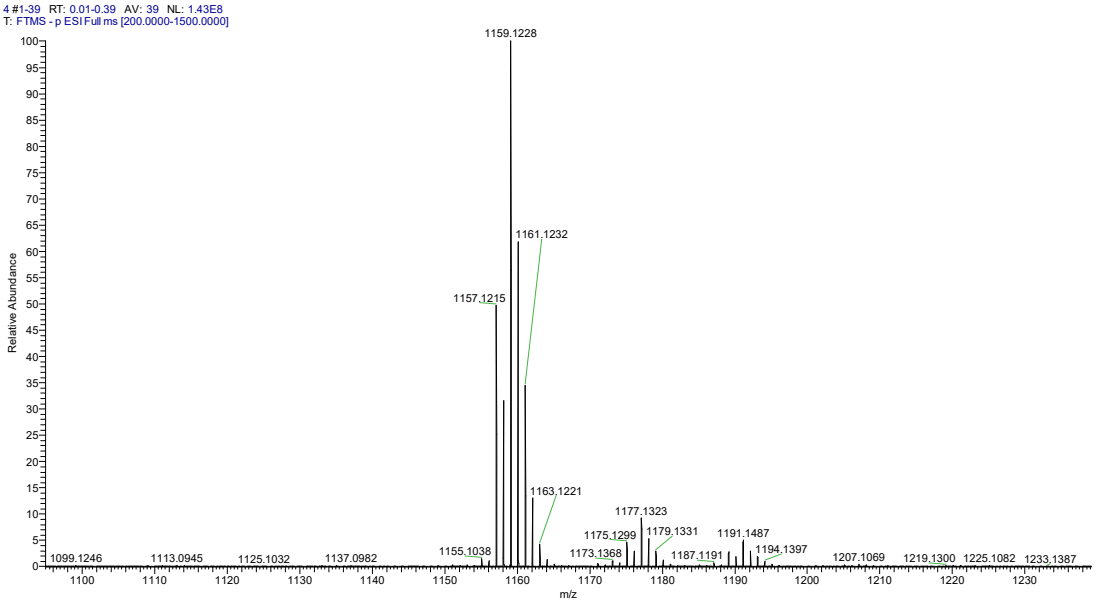

Figure S9. HRMS spectrum of **Ir3**.

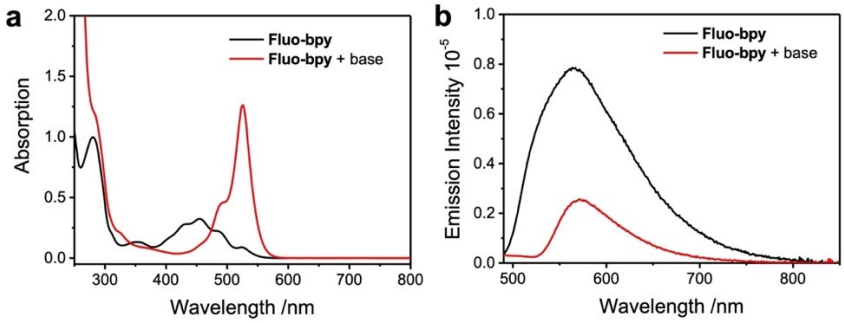

Figure S10. (a) UV-vis absorption spectra of the ligand **Fluo-bpy** in acetonitrile with (red line)/ without excess base (black line). (b) Emission spectra of the ligand **Fluo-bpy** in acetonitrile with (red line)/ without excess base (black line). Conc. = 2.5×10^{-5} M.

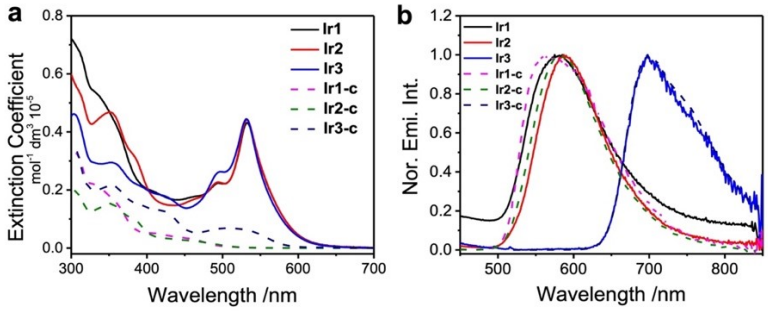

Figure S11. (a) UV-vis spectra of **Ir1**–**Ir3** and **Ir1-c**–**Ir3-c**. (b) Normalized emission spectra of **Ir1**–**Ir3** and **Ir1-c**–**Ir3-c** in acetonitrile solution at room temperature.

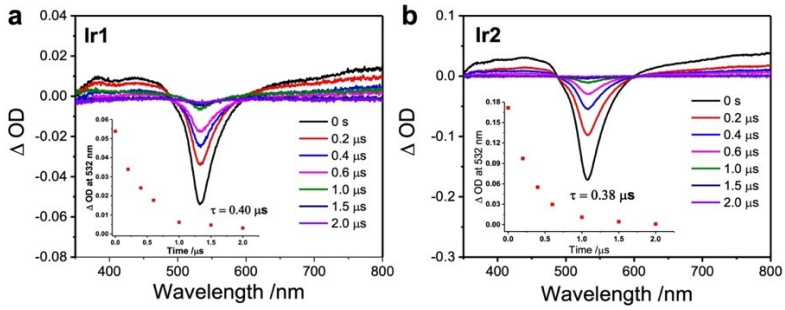

Figure S12. Transient absorption difference spectra of (a) **Ir1** and (b) **Ir2** in degassed acetonitrile (1 μL triethylamine) at 298K. Conc. = 2.5×10^{-5} M.

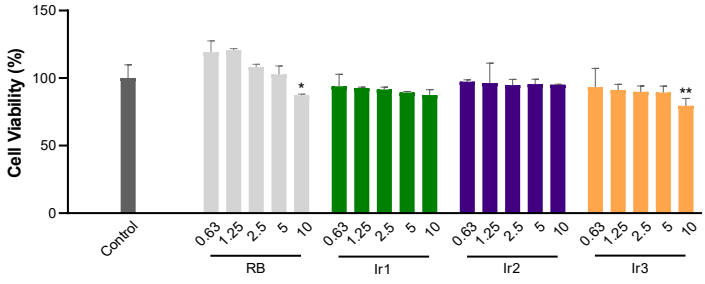

Figure S13. The dark cytotoxicity of **Ir1**–**Ir3** at varied concentrations. (*$p < 0.05$, **$p < 0.01$ *vs.* the Control group, n = 3)

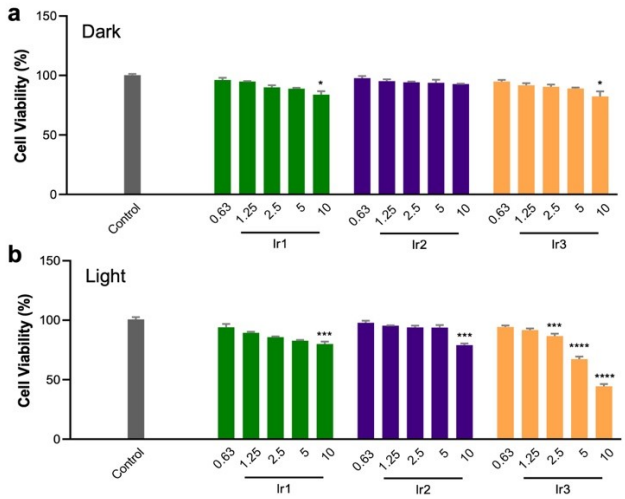

Figure S14. (a) The dark cytotoxicity of **Ir1**–**Ir3** at varied concentrations under hypoxic condition. (b) The light cytotoxicity of **Ir1**–**Ir3** at varied concentrations under hypoxic condition. (*$p < 0.05$, **$p < 0.01$ *vs.* the Control group, n = 3)

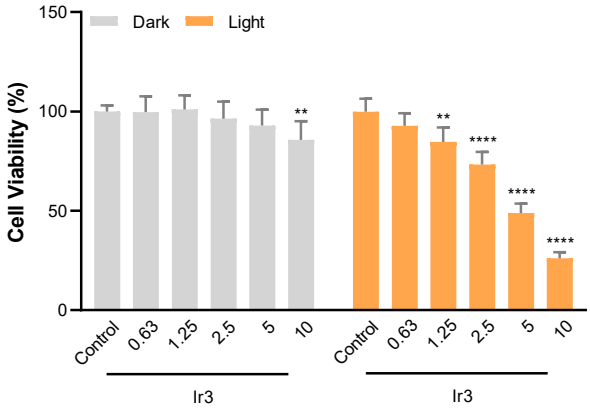

Figure S15. The dark and light cytotoxicity results of Ir3 on L929 cells. (**$p < 0.01$, ****$p < 0.0001$ *vs*. the Control group, n = 3)

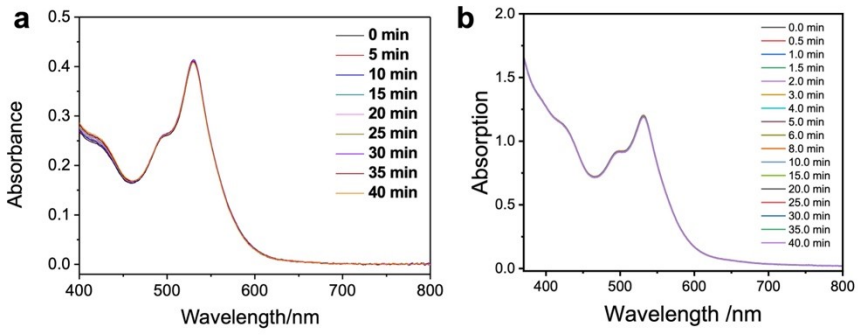

Figure S16. The light stability of **Ir3** under varied light-treatment time. (a) white light (5 mW cm^{-2}); (b) continuous laser (λ_{ex} = 650 nm, 20 mW cm^{-2}).

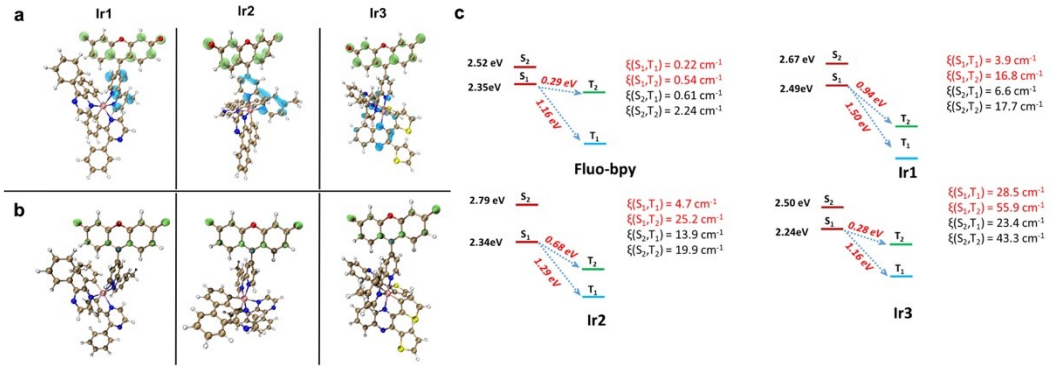

Figure S17. (a) Distribution of Frontier Molecular Orbitals (HOMO: green, LUMO: blue) of **Ir1**–**Ir3** at the Ground State. (b) Plots of spin density (isovalue = 0.02) of the T_1 state of **Ir1**–**Ir3.** (c) Calculated SOC values of **Fluo-bpy** and **Ir1**–**Ir3**.

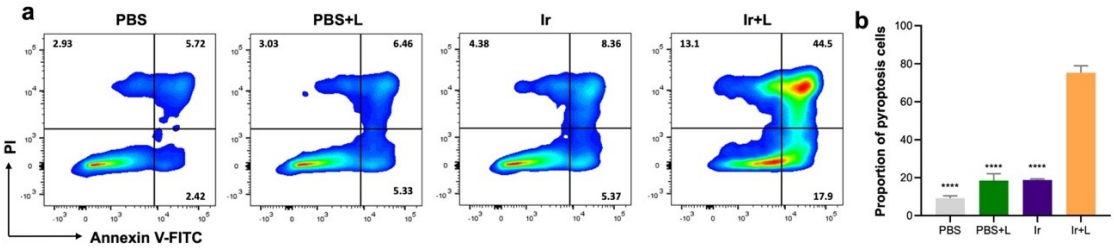

Figure S18. The flow cytometry results of pyroptosis induced by PDT.

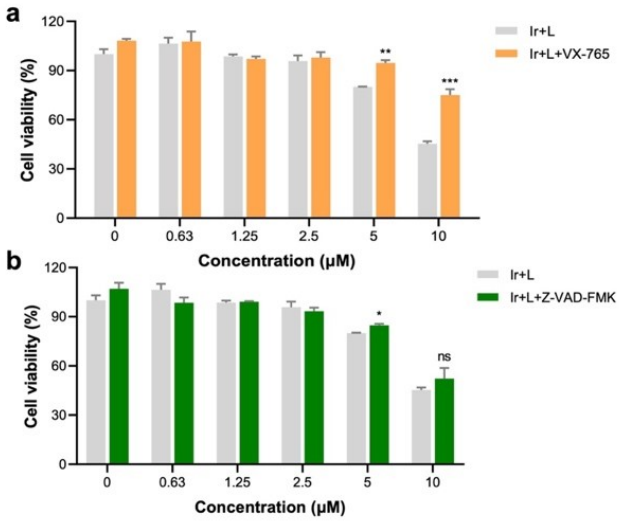

Figure S19. The light cytotoxicity of **Ir3** on RM-1 cells that pre-treated with Caspase-1 inhibitor VX-765 (10 μM) or apoptosis-related inhibitor Z-VAD-FMK (10 μM).

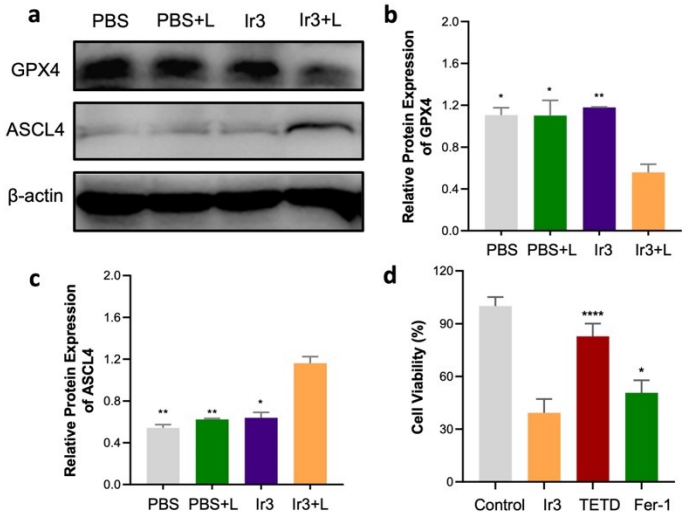

Figure S20. Ferroptosis pathway study. (a) The expression of GPX4 and ASCL4 post-treatment with PBS or Ir3, with or without light irradiation. Quantitative analysis of the Western blotting results in (b) GPX4, (c) ASCL4. (*$p < 0.05$, **$p < 0.01$ *vs*. the Ir3+L group, n = 3). (d) The light cytotoxicity of Ir3 on RM-1 cells that pre-treated with pyroptosis-related inhibitor TETD (10 μM) or ferroptosis-related inhibitor Fer-1 (10 μM). (*$p < 0.05$, ****$p < 0.0001$ *vs*. the Ir3 group, n = 3).

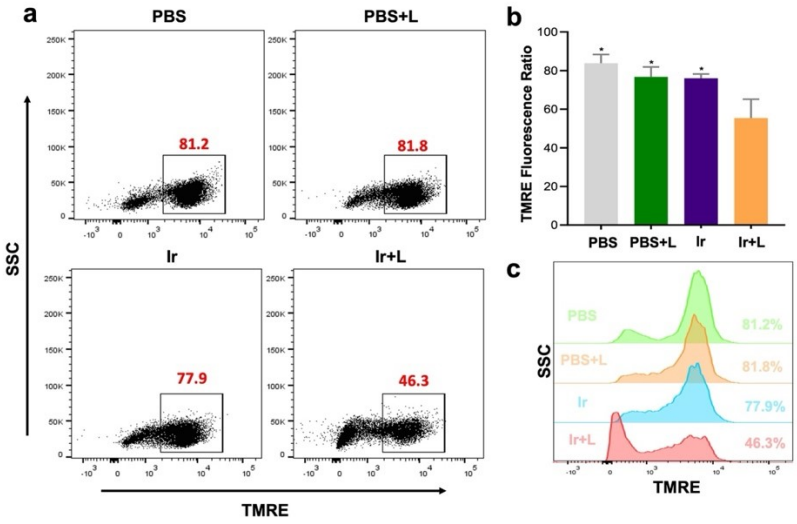

Figure S21. The depolarization of mitochondria caused by **Ir3**-induced pyroptosis.

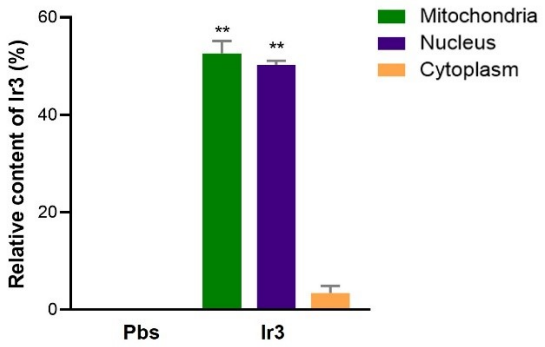

Figure S22. The subcellular organelle distribution of Ir3 by ICP-MS. (**$p < 0.01$ *vs.* the Control group, n = 3)

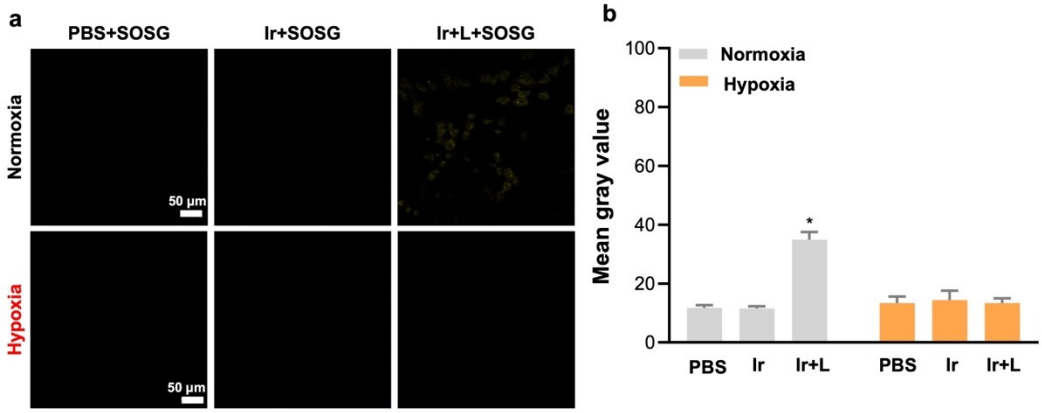

Figure S23. (a) Confocal imaging of intra-cellular singlet oxygen after the treatment of Ir3+light under normoxia (21% O_2) or hypoxia (2% O_2). (b) Quantitative results of confocal imaging.

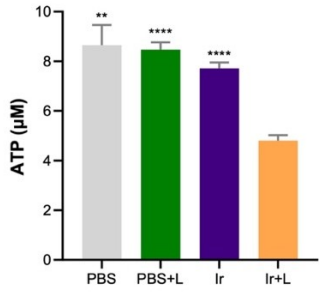

Figure S24. ELISA results of intracellular ATP expression from different groups.

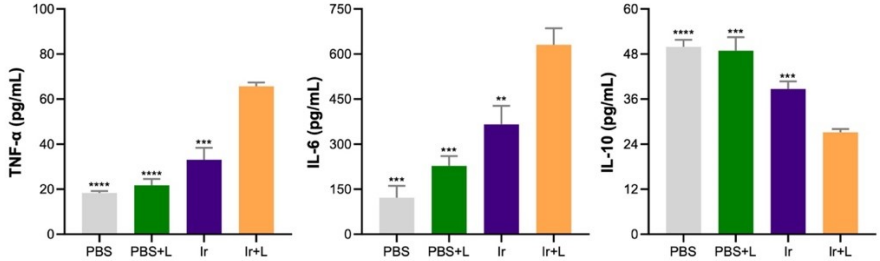

Figure S25. ELISA results of TNF-α, IL-6 and IL-10 in the supernatant of DCs.

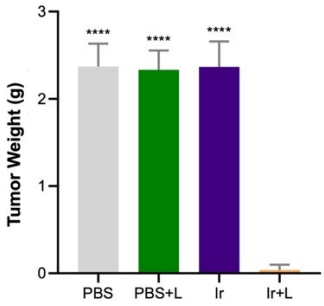

Figure S26. The tumor weight data of mice in different groups on day 10.

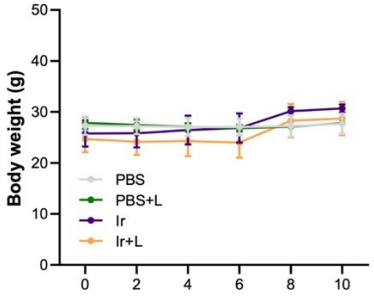

Figure S27. The body weight data of mice in different groups after treatments.

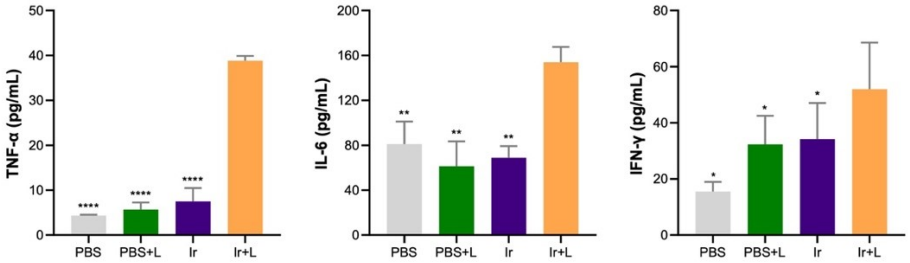

Figure S28. The secretion of proinflammatory cytokines (TNF-α, IL-6, and IFN-γ) were detected to verify the activation of T cells immunity.

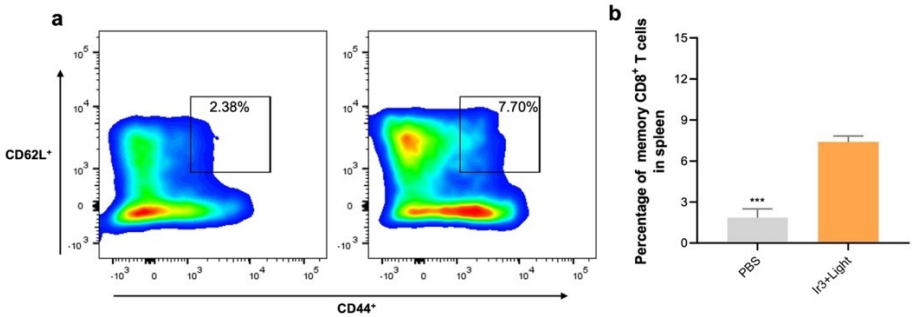

Figure S29. The effector memory T cells proportion in the spleen of the Ir+L group and control group.

Table S1. Photophysical data of **Ir1**–**Ir3**.

	$\lambda_{abs}{}^{a}$ [nm]	ε^{b} [dm^3 mol^{-1} cm^{-1}]	$\lambda_{em}{}^{a,c}$ [nm]	$\Phi_{Lum}{}^{d}$ [%]	τ^{e} [μs]

Ir1	495, 532	22430, 43155	580	0.086	0.40
Ir2	495, 532	22690, 44200	588	0.089	0.38
Ir3	495, 532	24000, 44380	700	0.075	0.45

[a]Conc. = 2.5 × 10^{-5} M. [b]Molar extinction coefficient at the absorption maxima. [c]Emission in degassed acetonitrile solution. [d]Absolute luminescence quantum yield. [e]Transient absorption lifetime.